metals

MDPI

Article

First-Principles Study of Elastic Properties and Electronic Properties of Al-Ni-Ce Ternary Intermetallic Compounds

Ying Ling [1,2], Wenjie Hu [1,2], Jiabin Wang [1,2] and Hong Yan [1,2,*]

[1] School of Advanced Manufacturing, Nanchang University, Nanchang 330031, China; 412400220102@email.ncu.edu.cn (Y.L.); 412400220125@email.ncu.edu.cn (W.H.); 402400230067@email.ncu.edu.cn (J.W.)
[2] Key Laboratory of Light Alloy Preparation & Processing, Nanchang University, Nanchang 330031, China
* Correspondence: hyan@ncu.edu.cn; Tel.: +86-0791-8396-9622

Abstract: The materials of the Al-Ni-Ce ternary system have promising application potential in additive manufacturing, and the systematic study of Al-Ni-Ce IMCs is an important part of the design and performance development of Al-Ni-Ce alloys. In this paper, the mechanical properties and electronic properties of seven major Al-Ni-Ce IMCs are studied using first-principles calculations, and the differences in their mechanical properties are discussed. The enthalpy of formation and cohesion energy of the Al-Ni-Ce IMCs showed that $Ce_4Al_{23}Ni_6$ had the highest enthalpy of formation and cohesion energy, which were −49.57 kJ/mol and −4.47 kJ/mol, respectively. This demonstrated that all Al-Ni-Ce IMCs had excellent thermodynamic stability. The elastic modulus calculation of the Al-Ni-Ce IMCs showed that the Young's modulus of $CeAl_3Ni_2$ was the largest at 178.15 GPa, the bulk modulus of $CeAlNi_4$ was the largest at 125.78 GPa, and the shear modulus of $CeAlNi_2$ was the largest at 62.53 GPa. This proved that among the Al-Ni-Ce IMCs, $CeAl_3Ni_2$ had the greatest stiffness, $CeAlNi_4$ had the strongest resistance to uniform deformation, and $CeAl_3Ni_2$ had the strongest resistance to plastic deformation. The electronic density of states of Al-Ni-Ce IMCs was analyzed, and the results showed that the main bonding types of Al-Ni-Ce IMCs were metallic and covalent bonds. This work can provide a theoretical basis for the material design and development of the Al-Ni-Ce ternary system.

Keywords: first-principles calculations; intermetallic; Al-Ni-Ce; mechanical properties; electronic properties

Citation: Ling, Y.; Hu, W.; Wang, J.; Yan, H. First-Principles Study of Elastic Properties and Electronic Properties of Al-Ni-Ce Ternary Intermetallic Compounds. *Metals* **2023**, *13*, 1921. https://doi.org/10.3390/met13121921

Academic Editors: Tomasz Czujko and Guy Makov

Received: 19 October 2023
Revised: 19 November 2023
Accepted: 20 November 2023
Published: 22 November 2023

1. Introduction

Al alloys are widely used in industrial manufacturing fields such as aerospace and vehicle engineering due to their ease of processing, excellent strength-to-mass ratio, and unique mechanical properties [1,2]. A large number of long-range ordered intermetallic compounds (IMCs) are present in Al alloys, and their characteristics clearly distinguish them from the Al matrix [3]. Although the brittleness exhibited by IMCs can limit the application of IMCs, understanding the nature of IMCs in Al alloying systems is nonetheless extremely important for the strengthening mechanisms and performance enhancement of Al alloys.

In recent years, researchers have found that Al-Ni-Ce alloys have a narrow freezing range similar to that of Al-Si10-Mg alloys, which has immeasurable potential for additive manufacturing [4]. There are also some correlations between the IMCs of the Al-Ni-Ce system and the creep properties of Al-Ni-Ce alloys. Michi et al. [5] found that Al-Ni-Ce alloys to which a small amount of Mn was added exhibited significant creep resistance due to the high-volume fraction of IMCs in the eutectic microstructure. The results of Wu et al. [6] showed that creep strengthening of Al-Ni-Ce alloys arises from load transfer from the Al matrix to IMCs. Therefore, the study of Al-Ni-Ce IMCs is valuable for the application development and strengthening mechanism of Al-Ni-Ce alloys.

According to the papers we reviewed, Al-Ni-Ce IMCs are more studied in terms of thermodynamics. Wang et al. [7] calculated the enthalpies of formation of Al-Ni-Ce IMCs, as well as isothermal cross sections and liquid-phase line projections at 1073 K and 773 K, to refine the thermodynamic parameters of the ternary equilibrium phase of Al-Ni-Ce. Tang et al. [8] studied the phase equilibria of the Al-Ce-Ni system in the region of 0–33.3 at. % Ce at 800 °C and systematically investigated the ternary phases and their lattice parameters as a function of the solid solution composition, and based on the results, corrected the modified partial isothermal cross-section of the Al-Ce-Ni system at 800 °C. Wang et al. [9] investigated the effect of elemental Ce on the structural, elastic, and electronic properties of NiAl alloy structures and showed that Ce led to lattice distortion of NiAl and increased the hardness and ductility of NiAl. Delsante et al. [10] studied the peculiarities of the formation of aluminum-rich phases in the Ce-Ni-Al ternary system, and combined with microstructure and X-ray diffraction, the existence of $Ce_4Ni_6Al_{23}$ and $CeNiAl_4$ was confirmed. These studies have continuously improved the thermodynamic parameters of Al-Ce-Ni IMCs. However, the load transfer between Al-Ce-Ni IMCs and the Al matrix and the mechanical properties of Al-Ce-Ni IMCs are closely related. Therefore, Al-Ce-Ni IMCs' phase stability, mechanical properties, and other aspects need to be further studied.

First-principles calculations based on density–functional theory have been used to obtain information at the atomic and electronic microscopic level, which provided a unique advantage in studying the crystal structure, mechanical properties, and electronic properties of IMCs [11–13]. Therefore, first-principles calculations have become increasingly popular among researchers in the study of IMCs [14–16]. In this paper, seven major IMCs ($CeAl_4Ni$, $Ce_4Al_{23}Ni_6$, $CeAl_5Ni_2$, $CeAl_3Ni_2$, $CeAlNi_4$, $CeAl_2Ni$, and CeAlNi) have been investigated using first-principles calculations in the Al-Ni-Ce system, and their distributions in the Al-Ni-Ce system are presented in Figure 1 [17,18]. Their crystal structures, enthalpy of formation and cohesion energy, elastic properties, and electronic properties are investigated, and these parameters can reflect the stability of the phase structure, the stability and mechanical properties under stress conditions, and the bonding characteristics of Al-Ni-Ce IMCs. This study is expected to provide a theoretical basis for the development of creep-strengthening mechanisms and properties of Al-Ni-Ce alloys.

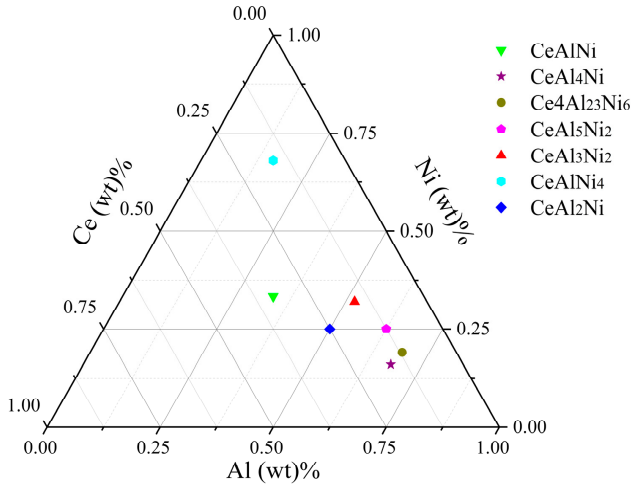

Figure 1. Distribution of Al-Ni-Ce ternary intermetallic compounds in phase diagrams.

2. Calculation Method

All calculations in this paper were performed using the open-source academic version of the CASTEP program [19]. The electron exchange correlation was investigated using the Generalized Gradient Approximation (GGA) with PBE generalization [20]. The ultrasoft pseudopotential was adopted because it can be calculated at a lower cutoff energy. The Kohn–Sham equation was solved using the self-concordant field (SCF) to reach the ground

state through an electron minimization process [21], setting the energy tolerance of the SCF to 5.0×10^{-6} eV/atom. During the calculation process, the electronic configurations of Ce-4f5s5p5d6s, Ni-3d84s2, and Al-3s2s3p were taken as the valence electrons. The structure optimization of the equilibrium crystals was carried out through the BFGS method, with the total energy change per atom and the force convergence tolerance set to 5.0×10^{-5} eV/atom and 0.01 eV/Å, respectively. The crystal structure of Al-Ni-Ce IMCs is shown in Figure 2. The cutoff energies of $CeAl_2Ni$, $CeAl_5Ni_2$, $CeAlNi_4$, CeAlNi, $CeAl_3Ni_2$, $Ce_4Al_{23}Ni_6$, and $CeAl_4Ni$ were all set to 500 eV, and the k-points were set to $12 \times 4 \times 8$, $12 \times 6 \times 3$, $10 \times 6 \times 12$, $4 \times 4 \times 8$, $6 \times 6 \times 8$, $4 \times 12 \times 4$, and $12 \times 4 \times 9$, respectively.

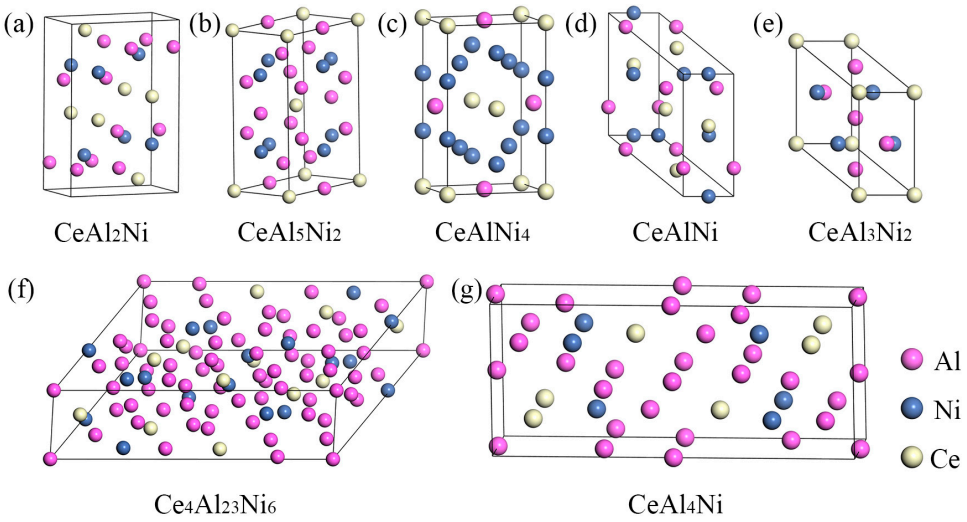

Figure 2. Crystal structure of Al-Ni-Ce intermetallic compounds. (**a**) $CeAl_2Ni$; (**b**) $CeAl_5Ni_2$; (**c**) $CeAlNi_4$; (**d**) CeAlNi; (**e**) $CeAl_3Ni_2$; (**f**) $Ce_4Al_{23}Ni_6$; (**g**) $CeAl_4Ni$.

3. Results and Discussion

3.1. Crystal Structure

The Al-Ni-Ce IMCs studied have a total of three different crystal systems. Among them, $CeNi_2Al_3$ and CeNiAl belong to the hexagonal crystalline system, with P6/mmm and P62m space groups, respectively. $CeNiAl_4$, $CeNi_2Al_5$, $CeNi_4Al$, and $CeNiAl_2$ all belong to the orthorhombic crystal system, $CeNiAl_4$, $CeNi_4Al$, and $CeNiAl_2$ all belong to the Cmmm space group, and $CeNi_2Al_5$ belongs to the Immm space group. $Ce_4Ni_6Al_{23}$ is a monoclinic crystal system with a C2/m space group. The crystal constants of Al-Ni-Ce IMCs were calculated, and the results of the calculations and other papers' comparative references are presented in Table 1. The calculated results are derived from the equilibrium lattice parameters obtained after each cell geometry optimization. The crystal constants of the Al-Ni-Ce IMCs are compared with the experimental values and are close to the experimental values with the maximum and minimum error ranges of 2.6% and 0.49%, respectively.

In addition, the volume and density of the Al-Ni-Ce IMCs were taken separately and analyzed. Figure 3 presents the relationship between the volume and density of Al-Ni-Ce IMCs and the Al, Ni, and Ce contents. The volume contour distribution of the Al-Ni-Ce system is shown in Figure 3a. It can be seen that the larger region of Al-Ni-Ce is mainly concentrated on the side of Al and Ce, and $CeAl_2Ni$, $CeAl_3Ni_2$, $CeAl_4Ni$, $CeAl_5Ni_2$, CeAlNi, and $Ce_4Al_{23}Ni_6$ are located in this region. However, there are small protruding areas at the Ni end, and $CeAlNi_4$ is present around it. The density contours of the Al-Ni-Ce system are shown in Figure 3b. It can be seen that the density of the Al-Ni-Ce ternary system is significantly affected by Al, and the lower the Al content, the greater the density. Combining the two parameters of volume and density, Al atoms have an important contribution to the lightening of Al-Ni-Ce IMCs.

Table 1. Lattice constants of Al-Ni-Ce intermetallic compounds.

Crystal	Lattice Constant (Å)			Volume (Å^3)	Density (g/cm^3)	Reference
	a	b	c			
$CeAl_2Ni$	4.07	10.61	6.92	299.07	5.61	This work
$CeAl_3Ni_2$	5.29	5.29	4.04	98.24	5.72	This work
	5.25	5.25	4.02	95.88	5.86	Exp. [22]
$CeAl_4Ni$	4.12	15.61	6.61	426.38	4.77	This work
	4.10	15.57	6.61	421.86	4.83	Exp. [17]
$CeAl_5Ni_2$	3.98	7.04	9.54	267.84	4.86	This work
	3.98	7.00	9.52	265.20	4.91	Exp. [23]
CeAlNi	6.96	6.96	4.01	168.50	6.67	This work
	6.87	6.87	4.02	164.10	6.85	Exp. [24]
$CeAlNi_4$	5.06	8.38	4.08	173.66	7.68	This work
$Ce_4Al_{23}Ni_6$	16.04	4.12	18.30	1113.15	4.57	This work
	16.00	4.12	18.31	1107.59	4.60	Exp. [25]

Exp. Experiment.

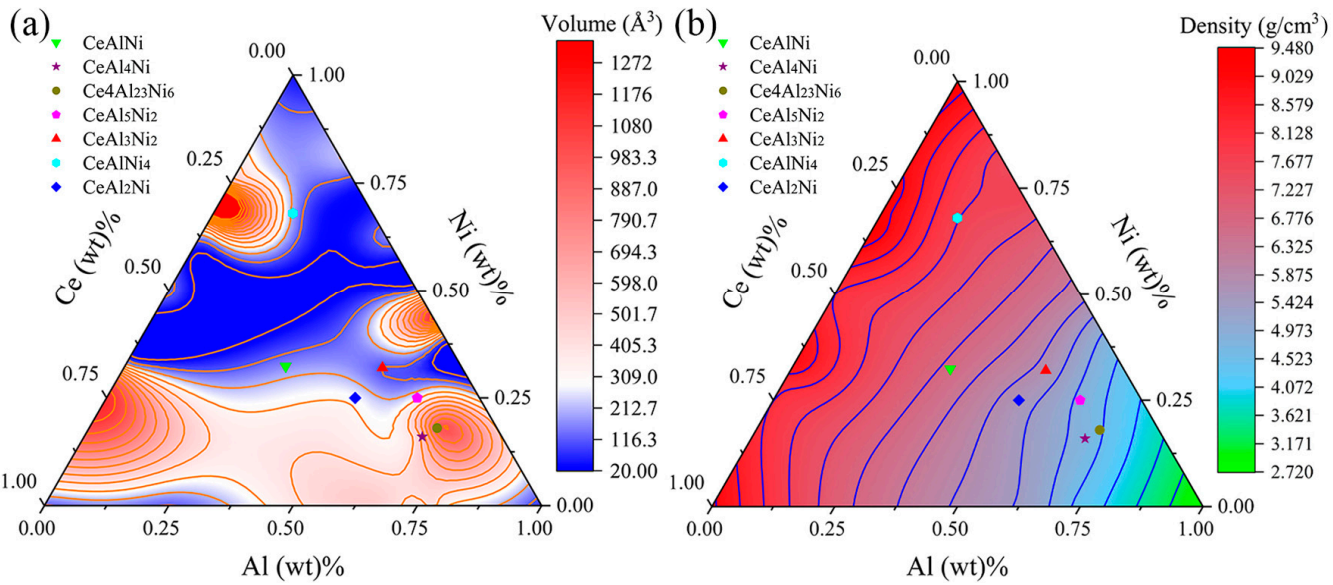

Figure 3. Volume and density distribution of Al-Ni-Ce intermetallic compounds. (**a**) Volume contour; (**b**) density isometric.

3.2. Enthalpy of Formation and Cohesion Energy

The calculation of the enthalpy of formation and cohesion energy allows the phase stability of Al-Ni-Ce IMCs to be analyzed from an energetic point of view. The enthalpy of formation ($\Delta H_f(Al_mNi_nCe_l)$) is equal to the energy of formation ($E_f(Al_mNi_nCe_l)$) for Al-Ni-Ce IMCs in the computational environment without taking into account temperature and air pressure [26], specifically expressed as

$$\Delta H_f(Al_mNi_nCe_l) = E_f(Al_mNi_nCe_l) \tag{1}$$

The calculation of the enthalpy of formation and the cohesion energy can be expressed as [27]

$$\Delta H_{formation} = \frac{E_{total}^{Al_mNi_nCe_l} - mE_{solid}^{Al} - nE_{solid}^{Ni} - lE_{solid}^{Ce}}{m+n+l} \tag{2}$$

$$E_{cohesive} = \frac{E_{total}^{Al_mNi_nCe_l} - mE_{atom}^{Al} - nE_{atom}^{Ni} - lE_{atom}^{Ce}}{m+n+l} \tag{3}$$

where $E_{total}^{Al_mNi_nCe_l}$ denotes the total energy; E_{solid}^{Al}, E_{solid}^{Ni}, and E_{solid}^{Ce} denote the energies of individual atoms in the face-centered cubic (FCC) structure of Al, Ni, and Ce monomers; E_{atom}^{Al}, E_{atom}^{Ni}, and E_{atom}^{Ce} denote the energies of individual atoms in the free states of Al, Ni, and Ce; and m, n, and l denote the number of atoms in the Al-Ni-Ce IMCs that correspond to Al, Ni, and Ce, respectively.

The enthalpy of formation is defined as the difference between the total energy of a compound and the energy of its constituent elements in a steady state. The cohesion energy is defined as the work required when crystals break down into free atoms. The enthalpy of formation and cohesion energy of Al-Ni-Ce IMCs are shown in Table 2. The calculation results of the enthalpy of formation showed that the absolute enthalpy of formation of $CeAl_3Ni_2$ is the maximum, indicating that it has the strongest alloying ability, while the opposite is true for $Ce_4Al_{23}Ni_6$. The alloying ability of the seven Al-Ni-Ce IMCs was in the order of $CeAl_3Ni_2$ > $CeAl_5Ni_2$ > CeAlNi > $CeAl_4Ni$ > $CeAl_2Ni$ > $CeAlNi_4$ > $Ce_4Al_{23}Ni_6$. The calculated results are in good agreement with the experimental results, which confirms the rationality and reliability of the calculation method. The calculated enthalpy of formation and cohesion energy of Al-Ni-Ce IMCs are less than 0, which indicates that the process of combining these atoms to form the compound is exothermic. The thermodynamic stability of IMCs is closely related to the enthalpy of formation and cohesion energy, and the lower the enthalpy of formation and cohesion energy, the better the thermodynamic stability. Therefore, Al-Ni-Ce IMCs have great thermal stability.

Table 2. Enthalpy of formation and cohesion energy of Al-Ni-Ce intermetallic compounds.

Crystal	Enthalpy of Formation (kJ/mol)		Cohesion Energy (kJ/mol)
	Present Work	Reference [9]	
$CeAl_2Ni$	−52.2	−55.7	−4.66
$CeAl_3Ni_2$	−60.52	−61.5	−4.77
$CeAl_4Ni$	−52.88	−53.6	−4.52
$CeAl_5Ni_2$	−57.06	−56.6	−4.62
CeAlNi	−56.16	−56.2	−4.84
$CeAlNi_4$	−51.40		−5.03
$Ce_4Al_{23}Ni_6$	−49.57	−48.3	−4.47

Due to the particularity of rare earth atoms, the enthalpy of formation and cohesion energy of Al-Ni-Ce IMCs will be affected by the content ratio of Ce atoms. To further illustrate the relationship between the enthalpy of formation and cohesion energy of Al-Ni-Ce IMCs and the Ce atom under vacuum conditions (0 K, 0 Pa), the relationship between the enthalpy of formation and the cohesion energy and the content of Ce atoms is shown in Figure 4. The relationship between the enthalpy of formation of Al-Ni-Ce IMCs and the Ce content is shown in Figure 4a. Clearly, the enthalpy of formation is higher on the side with less Ce content. According to other works [28], the solubilization of Ce in Al-Ni IMCs is difficult. Therefore, the content of Ce is less, which is more conducive to the alloying of Al-Ni-Ce IMCs. The relationship between the cohesion energy and Ce content of Al-Ni-Ce IMCs is shown in Figure 4b, and the absolute value of cohesion energy gradually increases with the increase in Ce content. This indicates that the presence of Ce atoms strengthens the association of Al-Ni-Ce IMCs, which are difficult to decompose into free atoms.

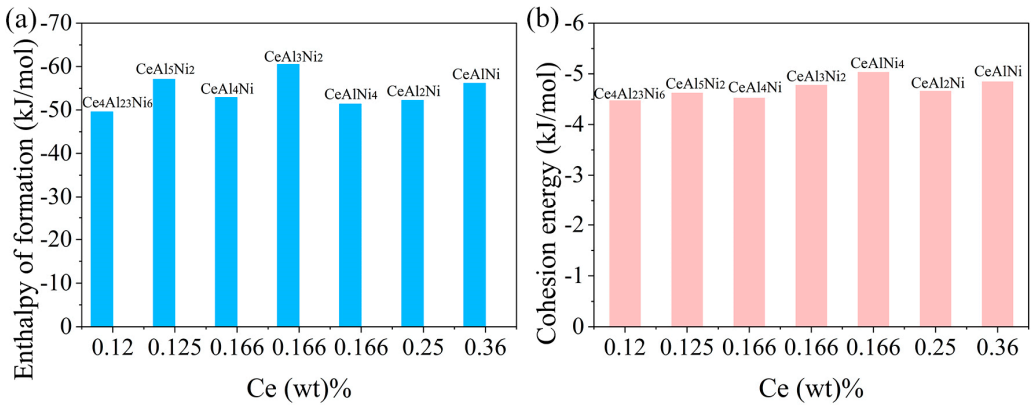

Figure 4. The calculated enthalpies of formation and cohesion energy plotted as a function of mole fraction of Ce for Al-Ni-Ce IMCs. (**a**) Enthalpy of formation; (**b**) cohesion energy.

3.3. Elastic Constants and Elastic Modulus

3.3.1. Elastic Constants

The elastic stiffness constant of the crystal, C_{ij}, reflects the deformation capacity of the crystal under stress conditions, where C_{11} and C_{12} denote transverse deformation and C_{44} denotes longitudinal deformation, and the larger the value, the better the mechanical properties. The elastic stiffness constant C_{ij} can be expressed as [29]

$$C_{ij} = \frac{1}{V_0}\left(\frac{\partial^2 E}{\partial \varepsilon_i \partial \varepsilon_j}\right) \tag{4}$$

where E is the energy of the crystal, V_0 is its equilibrium volume, and ε denotes a strain. The C_{ij} reflects the mechanical stability of the crystal, and the stability criterion is determined differently for different crystal systems. The calculated elastic stiffness constants of Al-Ni-Ce IMCs are presented in Table 3. From the calculation results, it can be seen that the elastic stiffness constants of the Al-Ni-Ce IMCs depend on the stability determination criterion of the crystalline systems they correspond to, which indicates that the Al-Ni-Ce IMCs can be mechanically stabilized.

For the orthorhombic crystals [30] ($CeAl_2Ni$, $CeAlNi_4$, $CeAl_5Ni_2$, $CeAl_4Ni$):

$$\left\{\begin{array}{c} C_{ii} > 0;\ i = 1 \sim 6 \\ C_{11} + C_{22} + C_{33} + 2(C_{12} + C_{13} + C_{23}) > 0 \\ C_{11} + C_{22} - 2C_{12} > 0 \\ C_{11} + C_{33} - 2C_{13} > 0 \\ C_{22} + C_{33} - 2C_{23} > 0 \end{array}\right\} \tag{5}$$

For the hexagonal crystals [31] ($CeAl_3Ni_2$, CeAlNi):

$$\left\{\begin{array}{c} C_{11} > 0;\ C_{44} > 0 \\ C_{11} - |C_{12}| > 0 \\ (C_{11} + C_{12})C_{33} - 2C_{13}^2 > 0 \end{array}\right\} \tag{6}$$

For the monoclinic crystal [32] ($Ce_4Al_{23}Ni_6$):

$$\left\{\begin{array}{c} C_{ii} > 0;\ i = 1 \sim 6 \\ C_{33}C_{55} - C_{35}^2 > 0;\ C_{44}C_{66} - C_{46}^2 > 0;\ C_{22}C_{33} - C_{23}^2 > 0 \\ C_{11} + C_{22}C_{33} + 2(C_{12} + C_{13}C_{23}) > 0 \\ C_{22}\left(C_{33}C_{55} - C_{35}^2\right) + 2\left(C_{23}C_{25}C_{35} - C_{25}^2C_{55} - C_{25}^2C_{33}\right) > 0 \\ 2\begin{bmatrix} C_{15}C_{25}(C_{33}C_{12} - C_{13}C_{23}) + \\ C_{15}C_{35}(C_{22}C_{13} - C_{12}C_{23}) + \\ C_{25}C_{35}(C_{11}C_{23} - C_{12}C_{13}) \end{bmatrix} - \begin{bmatrix} C_{15}^2(C_{22}C_{33} - C_{23}^2) + \\ C_{25}^2(C_{11}C_{33} - C_{13}^2) + \\ C_{35}^2\left(C_{11}C_{22} - C_{12}^2\right) + C_{35} \end{bmatrix} > 0 \end{array}\right\} \quad (7)$$

Table 3. The elastic constants of Al-Ni-Ce intermetallic compounds.

Crystal	Elastic Stiffness Constants C_{ij} (GPa)								
	C_{11}	C_{12}	C_{13}	C_{22}	C_{23}	C_{33}	C_{44}	C_{55}	C_{66}
$CeAl_2Ni$	154.57	60.98	87.28	104.54	59.92	127.28	40.50	84.35	27.40
$CeAl_3Ni_2$	191.95	58.62	69.05	191.95	70.41	219.68	80.51	80.28	68.85
$CeAl_4Ni$	171.92	38.14	68.39	177.88	48.02	413.69	59.63	87.25	61.29
$CeAl_5Ni_2$	175.27	71.30	46.44	176.63	79.34	153.36	52.36	62.71	87.54
CeAlNi	133.20	41.68	98.22	133.20	98.22	174.58	56.90	56.90	45.75
$CeAlNi_4$	196.67	81.84	88.45	198.76	79.57	241.93	40.67	85.79	47.51
$Ce_4Al_{23}Ni_6$	175.42	52.56	48.37	180.49	63.41	166.02	70.26	61.21	77.95

* $Ce_4Al_{23}Ni_6$ belongs to the monoclinic crystal system, and it is still necessary to add several elastic constants, which are C_{15} = 2.84; C_{25} = 9.53; C_{35} = −6.09; and C_{45} = 9.97.

3.3.2. Elastic Modulus

The Voigt–Reuss–Hill method [33] was used to calculate shear modulus (G) and bulk modulus (B) for Al-Ni-Ce IMCs. As with the elastic constants, different crystal systems correspond to different equations of the calculation.

For the orthorhombic crystals ($CeAl_2Ni$, $CeAlNi_4$, $CeAl_5Ni_2$, $CeAl_4Ni$):

$$\left\{\begin{array}{c} G_V = \frac{1}{15}[C_{11} + C_{22} + C_{33} + 3(C_{44} + C_{55} + C_{66}) - (C_{12} + C_{13} + C_{23})] \\ G_R = 15\left\{4\begin{bmatrix} C_{11}(C_{22} + C_{33} + C_{23}) + C_{22}(C_{33} + C_{13}) \\ +C_{33}C_{12} - C_{12}(C_{23} + C_{12}) \\ -C_{13}(C_{12} + C_{13}) - C_{23}(C_{13} + C_{23}) \end{bmatrix} \Big/ \Delta + 3\left(\frac{1}{C_{44}} + \frac{1}{C_{55}} + \frac{1}{C_{66}}\right)\right\}^{-1} \\ B_V = \frac{1}{9}[C_{11} + C_{12} + C_{33} + 2(C_{12} + C_{13} + C_{23})] \\ B_R = \Delta\begin{bmatrix} C_{11}(C_{22}+C_{33} - 2C_{23}) + C_{22}(C_{33} - 2C_{13}) - 2C_{33}C_{12} \\ +C_{12}(2C_{23} - C_{12}) + C_{13}(2C_{12} - C_{13}) + C_{23}(2C_{13} - C_{23}) \end{bmatrix}^{-1} \\ \Delta = C_{13}(C_{12}C_{23} - C_{13}C_{22}) + C_{23}(C_{12}C_{13} - C_{23}C_{11}) + C_{33}\left(C_{11}C_{22} - C_{12}^2\right) \end{array}\right\} \quad (8)$$

For the hexagonal crystals ($CeAl_3Ni_2$, CeAlNi):

$$\left\{\begin{array}{c} G_V = \frac{12(C_{44}+C_{66})+C_{11}+C_{12}+2C_{33}-4C_{13}}{30} \\ B_V = \frac{2(C_{11}+C_{12})+4C_{23}+C_{33}}{9} \\ G_R = \frac{5(C_{11}-C_{12})C_{44}}{4C_{44}+3(C_{11}-C_{12})} \\ B_R = \frac{C_{33}(C_{11}+C_{12})-2C_{13}^2}{C_{11}+C_{12}+2C_{33}-4C_{13}} \end{array}\right\} \quad (9)$$

For the monoclinic crystal ($Ce_4Al_{23}Ni_6$):

$$\left\{\begin{array}{c} G_V = \frac{1}{15}[C_{11}+C_{22}+C_{33}+3(C_{44}+C_{55}+C_{66})-(C_{12}+C_{13}+C_{23})] \\ G_R = 15\left\{4\left[\begin{array}{c}(C_{33}C_{55}-C_{35}^2)(C_{11}+C_{22}+C_{12})+\\(C_{23}C_{55}-C_{25}C_{35})(C_{11}-C_{12}-C_{23})+\\(C_{13}C_{35}-C_{15}C_{33})(C_{15}+C_{25})+\\(C_{13}C_{55}-C_{15}C_{35})(C_{22}-C_{12}-C_{23}-C_{13})+\\(C_{13}C_{25}-C_{15}C_{23})(C_{15}-C_{25})+f\end{array}\right]\Big/\Omega+3\left[g/\Omega+\frac{C_{44}+C_{66}}{C_{44}C_{66}-C_{46}^2}\right]\right\}^{-1} \\ B_V = \frac{1}{9}[C_{11}+C_{22}+C_{33}+2(C_{12}+C_{13}+C_{23})] \\ B_R = \Omega\left[\begin{array}{c}(C_{33}C_{55}-C_{35}^2)(C_{11}+C_{22}-2C_{12})+(C_{23}C_{55}-C_{25}C_{35})(2C_{12}-2C_{11}-C_{23})\\+(C_{13}C_{35}-C_{15}C_{33})(C_{15}-2C_{25})+(C_{13}C_{55}-C_{15}C_{35})\begin{pmatrix}2C_{12}+2C_{23}-C_{13}\\-2C_{22}\end{pmatrix}\\+2(C_{13}C_{25}-C_{15}C_{23})(C_{25}-C_{15})+f\end{array}\right]^{-1} \\ f = C_{11}(C_{22}C_{55}-C_{25}^2)-C_{12}(C_{12}C_{55}-C_{15}C_{25})+C_{15}(C_{12}C_{25}-C_{15}C_{22})+C_{25} \\ \times(C_{23}C_{35}-C_{25}C_{33}) \\ g = C_{11}C_{22}C_{33}-C_{11}C_{23}^2-C_{22}C_{13}^2-C_{33}C_{12}^2+2C_{12}C_{13}C_{23} \\ \Omega = 2\left[\begin{array}{c}C_{15}C_{25}(C_{33}C_{12}-C_{13}C_{23})+\\C_{15}C_{35}(C_{22}C_{13}-C_{12}C_{23})+\\C_{25}C_{35}(C_{11}C_{23}-C_{12}C_{13})\end{array}\right]-\left[\begin{array}{c}C_{15}^2(C_{22}C_{33}-C_{23}^2)+\\C_{25}^2(C_{11}C_{33}-C_{13}^2)+\\C_{35}^2(C_{22}C_{11}-C_{12}^2)\end{array}\right]+gC_{55} \end{array}\right\} \quad (10)$$

The average shear modulus (G) and bulk modulus (B), Young's modulus (E), and Poisson's ratio (ν) of Al-Ni-Ce IMCs were finally calculated as follows [34]:

$$\left\{\begin{array}{c} G = \frac{1}{2}(G_V+G_R) \\ B = \frac{1}{2}(B_V+B_R) \\ E = \frac{9BG}{3B+G} \\ \nu = \frac{3B-2G}{2(3B+G)} \end{array}\right\} \quad (11)$$

The calculated results of the Al-Ni-Ce IMCs elastic modulus are presented in Table 4. Pugh [35] proposed defining the brittleness of a material by the ratio of bulk modulus B to shear modulus, B/G. If the B/G ratio is greater than 1.75, the material is considered to be brittle. If the B/G ratio is greater than 1.75, the material is considered to be ductile, and if the B/G ratio is less than 1.75, the material is considered to be brittle. Based on the calculation of B/G ratios of Al-Ni-Ce intermetallic compounds, $CeAl_2Ni$, CeAlNi, and $CeAlNi_4$ were defined as ductile materials, while $CeAl_3Ni_2$, $CeAl_4Ni$, $CeAl_5Ni_2$, and $Ce_4Al_{23}Ni_6$ were defined as brittle materials.

Table 4. Elastic modulus of Al-Ni-Ce intermetallic compounds.

Crystal	Elastic Modulus				
	***E* (GPa)**	***B* (GPa)**	***G* (GPa)**	ν	***B*/*G***
$CeAl_2Ni$	100.73	86.71	38.55	0.30	2.24
$CeAl_3Ni_2$	178.15	111.08	72.26	0.23	1.53
$CeAl_4Ni$	152.02	89.07	62.53	0.21	1.42
$CeAl_5Ni_2$	148.16	99.12	59.22	0.25	1.67
CeAlNi	108.44	93.79	41.47	0.30	2.26
$CeAlNi_4$	151.89	125.78	58.47	0.29	2.15
$Ce_4Al_{23}Ni_6$	158.12	94.37	64.76	0.22	1.45

The shear modulus was used to evaluate the plastic deformation resistance and fracture behavior of the materials, with larger values indicating greater resistance to plastic deformation behavior. The calculated results in Table 4 show that the size order of the plastic deformation resistance of Al-Ni-Ce IMCs was $CeAl_3Ni_2$ > $Ce_4Al_{23}Ni_6$ > $CeAl_4Ni$ > $CeAlNi_4$ > $CeAl_5Ni_2$ > CeAlNi > $CeAl_2Ni$. This indicates that $CeAl_3Ni_2$ has the strongest resistance to plastic deformation of Al-Ni-Ce IMCs, while $CeAl_2Ni$ has the weakest resistance to plastic deformation. The bulk modulus reflects the ability of the material to resist uniform deformation. Calculations show that the order of magnitude of the ability of Al-Ni-Ce IMCs to resist uniform deformation is $CeAlNi_4$ > $CeAl_3Ni_2$ > $CeAl_5Ni_2$ > $Ce_4Al_{23}Ni_6$ > CeAlNi > $CeAl_4Ni$ > $CeAl_2Ni$. Li et al. [36] concluded that the bulk modulus of a crystal is determined by the ability of the chemical bonding to resist compressive forces, and the atom's electronegativity strength determines the size of the bulk modulus of the crystal. The electronegativity strength of Al-Ni-Ce IMCs is influenced by the rare earth element Ce atoms, so there is a correlation between the bulk modulus of Al-Ni-Ce IMCs and the composition of Ce atoms. Young's modulus is a physical measure of the stiffness of a material; the higher the Young's modulus the stiffer the material. The order of magnitude of the Young's modulus of Al-Ni-Ce IMCs is $CeAl_3Ni_2$ > $Ce_4Al_{23}Ni_6$ > $CeAl_4Ni$ > $CeAlNi_4$ > $CeAl_5Ni_2$ > CeAlNi > $CeAl_2Ni$. This shows that $CeAl_3Ni_2$ is the hardest of the Al-Ni-Ce intermetallic compounds, while $CeAl_2Ni$ has the lowest hardness. The magnitude of Poisson's ratio reflects the bonding force, which ranges from 0.25 to 0.45 for metallic materials [37]. The Poisson's ratios of the Al-Ni-Ce IMCs $CeAl_3Ni_2$, $CeAl_4Ni$, and $Ce_4Al_{23}Ni_6$ are all less than 0.25, which suggests that ionic bonding plays a dominant role in their bonding. The Poisson's ratios of $CeAl_2Ni$, $CeAl_5Ni_2$, CeAlNi, and $CeAlNi_4$ are all greater than 0.25, indicating that IMCs play a major role in their bonding.

The elastic modulus calculations of Al-Ni-Ce IMCs were compared with those of other materials, and the comparative results showed that the elastic modulus of Al-Ni-Ce IMCs was generally higher than that of Al-La IMCs [38], which proved that Al-Ni-Ce IMCs have more superior mechanical properties than some Al-RE binary IMCs. The shear modulus of Al-Ni-Ce IMCs was found to be generally higher than that of Al-Cu IMCs [39], which indicates that the Al-Ni-Ce system has a better plastic deformation capacity than the Al-Cu system. In comparison with the elastic modulus of the Mg-Al-Si IMCs [40], the elastic modulus of the Al-Ni-Ce IMCs was superior to that of the Mg-Al-Si system across the board. From these comparative results, it is clear that Al-Ni-Ce alloys have superior mechanical properties.

3.4. Anisotropic Elastic Properties

The spatial anisotropy coefficients of the modulus of elasticity can reflect the differences in the deformation of crystals subjected to forces in space. The contribution of the elastic modulus of the Al-Ni-Ce IMCs in all directions of space is shown in Figure 5. The elastic modulus can be presented using the visualization tool developed by Liao et al. [41].

When the three-dimensional image deviates from the spherical surface, it indicates that the elastic modulus behaves as anisotropies, and the larger the deviation, the more significant the anisotropies are. Therefore, as shown in Figure 5, the bulk modulus, shear modulus, Young's modulus, and Poisson's ratio of Al-Ni-Ce IMCs are all anisotropic. Among them, the most obvious anisotropy of bulk modulus is that of AlNiCe: the minimum value of bulk modulus is 49.0 GPa and the maximum value of bulk modulus is 31,315.5 GPa along the axial directions <−0.99, −0.16, 0> and <−0.47, 0, 0.88>, respectively. The largest anisotropy of Young's modulus is that of $CeAl_2Ni$: the minimum value of Young's modulus is 69.9 GPa and the maximum value is 164.1 GPa along the axial directions <0, 0, 1> and <−0.75, 0, −0.66>, respectively. The largest anisotropy of shear modulus is that of $CeAl_2Ni$: the minimum value of shear modulus is 29.1 GPa and the maximum value is 58.6 GPa along the axial directions <−0.75, 0, 0.66> and <0, 0, 1>, respectively. The largest Poisson's ratio is that of $CeAl_5Ni_2$: the minimum value of Poisson's ratio is 0.2 and the maximum value is 0.4 along the axial directions <0.84, 0.54, 0> and <0, −1, 0>, respectively. However,

the elastic anisotropy of the bulk modulus of $CeAl_3Ni_2$ and $CeAlNi_4$ is very similar, which indicates that there will be no distortion, crack, or other defects between $CeAl_3Ni_2$ and $CeAlNi_4$ under uniform stress conditions [42].

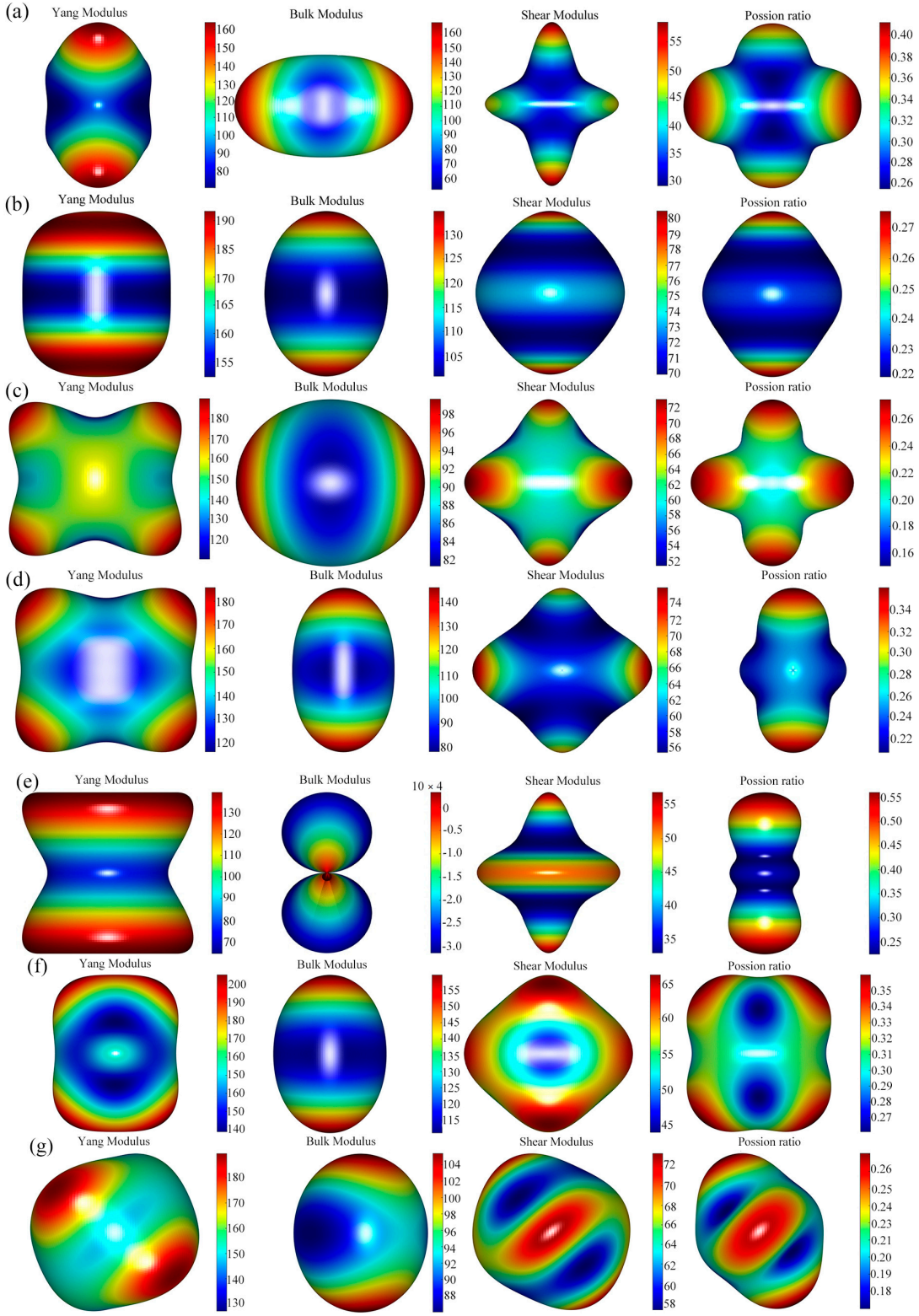

Figure 5. 3-D distributions of elastic constant anisotropy for Al-Ni-Ce intermetallic compounds. (**a**) $CeAl_2Ni$; (**b**) $CeAl_3Ni_2$; (**c**) $CeAl_4Ni$; (**d**) $CeAl_5Ni_2$; (**e**) CeAlNi; (**f**) $CeAlNi_4$; (**g**) $Ce_4Al_{23}Ni_6$.

The elasticity of each anisotropy can be expressed by the following equation [43]:

$$A_X = \begin{cases} \frac{X_{max}}{X_{min}}, & if\ sign(X_{max}) = sign(X_{min}) \\ \infty, & otherwise \end{cases} \quad (12)$$

When A_X = 1, this shows each isotropy, and the larger the value of A_X, the more drastic the crystal deformation. In addition, the elastic anisotropies of the Al-Ni-Ce IMCs were calculated separately and are presented in Table 5. The results of the elastic modulus anisotropy calculations are consistent with those in the 3D image. In addition, it can be seen from Table 5 that the elastic anisotropy of the Young's modulus of $CeAl_4Ni$ and $CeAlNi_4$ is the same, and the elastic anisotropy of the bulk modulus of $CeAl_4Ni$ and $Ce_4Al_{23}Ni_6$ is the same as that of the Poisson's ratio.

Table 5. The elastic modulus anisotropy A_X of Al-Ni-Ce intermetallic compounds.

Crystal	Elastic Modulus Anisotropy A_X			
	Young's Modulus	**Bulk Modulus**	**Shear Modulus**	**Poisson's Ratio**
$CeAl_2Ni$	2.34	3.26	2.01	1.33
$CeAl_3Ni_2$	1.18	1.33	1.15	1.64
$CeAl_4Ni$	1.72	1.22	1.42	1.50
$CeAl_5Ni_2$	1.59	1.96	1.38	2.00
CeAlNi	2.16	639.09	1.72	3
$CeAlNi_4$	1.72	1.43	1.51	1.33
$Ce_4Al_{23}Ni_6$	1.49	1.22	1.27	1.50

3.5. Partial Density of States

The PDOS is an excellent auxiliary tool for analyzing the electronic structure and chemical properties of materials. It can effectively reflect the bonding properties of IMCs. The results of the PDOS calculations for Al-Ni-Ce IMCs are presented in Figure 6. The results of the PDOS show that all Al-Ni-Ce IMCs have distinct metallic properties. In addition, the existence of resonance peaks near −17 eV for Ce and Al atoms with the same center of gravity proves the existence of covalent bonding properties between Al and Ce atoms. On the left side of the Fermi energy level, there is hybridization between the d-orbital electrons of the Ni atoms and the p-orbital electrons of the Al atoms, and the hybridization is more pronounced for $CeAlNi_4$ and $CeAl_3Ni_2$. There is hybridization of the f-orbital electrons of the Ce atoms and the p-orbital electrons of the Al atoms, in addition to the obvious hybridization of the s-orbital electrons of the Al atoms and the f-orbital electrons of the Ce atoms of $Ce_4Al_{23}Ni_6$. The waveform curves of these electronic orbital hybridizations have the same position, but different centers of gravity. This suggests that the Al-Ni-Ce IMCs also have a metallic bond. The presence of covalent bonds can enhance the strength of Al-Ni-Ce IMCs compared to pure metal bonds [44]. Therefore, the main bonding types of Al-Ni-Ce IMCs are covalent and metallic bonds with strong structural stability.

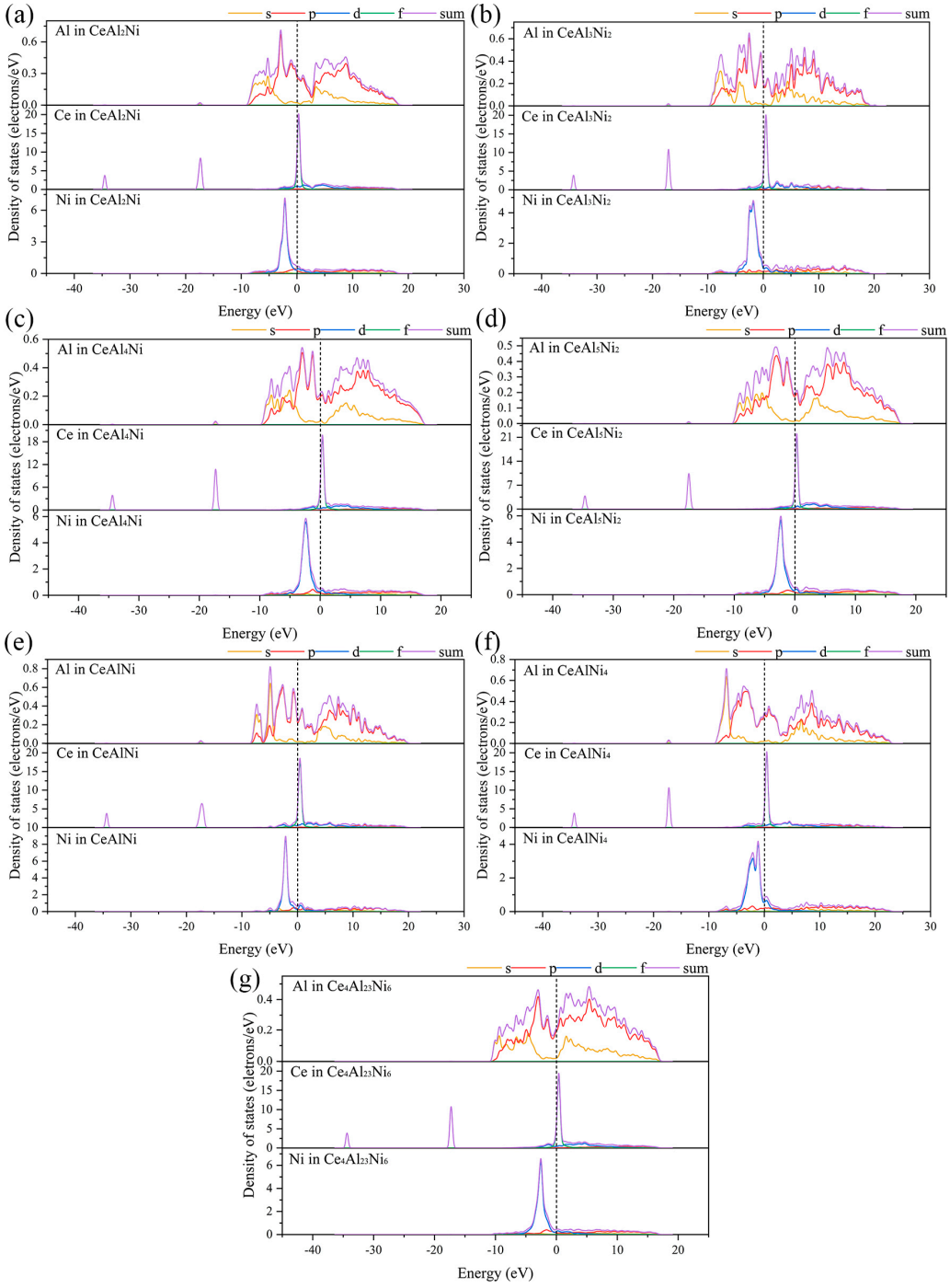

Figure 6. The partial density of states for Al-Ni-Ce intermetallic compounds. (**a**) $CeAl_2Ni$; (**b**) $CeAl_3Ni_2$; (**c**) $CeAl_4Ni$; (**d**) $CeAl_5Ni_2$; (**e**) CeAlNi; (**f**) $CeAlNi_4$; (**g**) $Ce_4Al_{23}Ni_6$.

4. Conclusions

The structure, thermodynamic properties, mechanical properties, and electronic structure of Al-Ni-Ce IMCs are systematically investigated in this work through first-principles calculations, and the conclusion is as follows:

1. The calculated results of lattice parameters were verified to be close to the experimental values.
2. The calculated enthalpy of formation and cohesion energy shows that the Al-Ni-Ce IMCs have good thermodynamic stability.

3. The elastic modulus results show that $CeAl_3Ni_2$ has the highest Young's modulus, $CeAlNi_4$ has the highest bulk modulus, and the Poisson's ratios of CeAlNi and $CeAl_2Ni$ are the highest.
4. The analysis of the Al-Ni-Ce IMCs modulus of elasticity showed that $CeAl_3Ni_2$, $CeAl_4Ni$, $CeAl_5Ni_2$, and $Ce_4Al_{23}Ni_6$ exhibited brittleness, while CeAlNi, $CeAlNi_4$, and $CeAl_2Ni$ exhibited toughness.
5. The results of elastic anisotropy analysis showed that the Young's modulus of $CeAl_4Ni$ and $CeAlNi_4$ was the same, the bulk modulus of $Ce_4Al_{23}Ni_6$ and $CeAl_4Ni$ was the same, and the Poisson's ratio of $CeAlNi_4$ and $CeAl_2Ni$ was the same.
6. The analysis of the fractional density of states reveals the prevalence of covalent and metallic bonds in the Al-NI-Ce IMCs.

Author Contributions: Conceptualization, Methodology, Investigation, Data curation, Writing—original preparation, Software, Y.L.; Visualization, Investigation, W.H.; Software, Investigation, J.W.; Funding acquisition, Supervision, Writing—review and editing, H.Y. All authors have read and agreed to the published version of the manuscript.

Funding: This research was funded by the National Natural Science Foundation of China (No. 51965040).

Institutional Review Board Statement: Not applicable.

Informed Consent Statement: Not applicable.

Data Availability Statement: The data presented in this study are available on request from the corresponding author. The data are not publicly available due to privacy.

Acknowledgments: The authors thank the National Natural Science Foundation of China (No. 51965040). [the Advanced Processing & Die CAD/CAE/CAM Research Laboratory of Nanchang University].

Conflicts of Interest: The authors declare no conflict of interest.

References

1. Peng, P.; Su, J.; He, Q.; Chen, R.; Chai, S.; Yu, D.; Dai, Q.; Lu, J. Solid-state bonding process induced highly synergistic mechanical properties of 6061 Al alloy joint by shear deformation. *J. Mater. Sci. Technol.* **2023**, *164*, 168–178. [CrossRef]
2. Tang, W.; Yang, X.; Wang, R.; Luo, T. Tailoring microstructure of additive friction stir-deposited Al–Mg alloy through post-processing deformation treatment for enhancing mechanical performance. *Mater. Sci. Eng. A* **2023**, *885*, 145632. [CrossRef]
3. Meng, Y.; Li, J.; Gao, M.; Chen, H. Preparation of Ni–Al intermetallic compounds by plasma arc melting deposition through double-wire feeding. *J. Mater. Res. Technol.* **2023**, *24*, 6174–6186. [CrossRef]
4. Perrin, A.E.; Michi, R.A.; Leonard, D.N.; Sisco, K.D.; Plotkowski, A.J.; Shyam, A.; Poplawsky, J.D.; Allard, L.F.; Yang, Y. Effect of Mn on eutectic phase equilibria in Al-rich Al-Ce-Ni alloys. *J. Alloys Compd.* **2023**, *965*, 171455. [CrossRef]
5. Michi, R.A.; Sisco, K.; Bahl, S.; Yang, Y.; Poplawsky, J.D.; Allard, L.F.; Dehoff, R.R.; Plotkowski, A.; Shyam, A.A. Creep-resistant additively manufactured Al-Ce-Ni-Mn alloy. *Acta Mater.* **2022**, *227*, 117699. [CrossRef]
6. Wu, T.; Plotkowski, A.; Shyam, A.; Dunand, D.C. Microstructure, and creep properties of cast near-eutectic Al–Ce–Ni alloys. *Mater. Sci. Eng. A* **2022**, *833*, 142551. [CrossRef]
7. Wang, H.; Li, Z.; Chen, Z.; Yang, B. Thermodynamic Optimization of the Ni-Al-Ce Ternary System. *J. Phase Equilib. Diffus.* **2016**, *37*, 222–228. [CrossRef]
8. Tang, C.; Du, Y.; Xu, H.H.; Xiong, W.; Zhang, L.J.; Zheng, F.; Zhou, H.Y. Experimental investigation of the Al–Ce–Ni system at 800 °C. *Intermetallics* **2008**, *16*, 432–439. [CrossRef]
9. Wang, Y.; He, J.; Yan, M.; Li, C.; Wang, L.; Zhou, Y. First-principles Study of NiAl Alloyed with Rare Earth Element Ce. *J. Mater. Sci. Technol.* **2011**, *27*, 719–724. [CrossRef]
10. Delsante, S.; Parodi, N.; Borzone, G. Effect of the Rare-Earth Addition (R = Ce, Sm) on the Phase Equilibria and Microstructure of Ni-Al Alloys. *J. Phase Equilib. Diffus.* **2014**, *35*, 421–428. [CrossRef]
11. Qiao, J.; Wu, F.; Chen, H.; Yang, Z.; Yan, R.; Bai, H.; Pan, F.; Lin, X. Investigation on electronic structures, elastic and thermodynamic properties of MNi3 (M=Be, Mg, Ca) intermetallic compound. *Phys. Rev. B Condens. Matter Mater. Phys.* **2023**, *668*, 415217. [CrossRef]
12. Cheng, Z.; Peng, Z.; Zhong, B.; Liu, H.; Lu, Z.; Zhu, S.; Liu, J. Substitution behavior of Cu doped into Fe3Si and its effect on the electronic structure and mechanical properties based on first-principles calculation. *Intermetallics* **2023**, *160*, 107918. [CrossRef]

13. Hao, L.Y.; Shen, S.K.; Zhang, S.L.; Liu, X.; Wang, Y.F.; Yang, K.J.; Fu, E.G. Ab-initio study on electronic, mechanical and dynamical properties of maraging steel containing coherent B2 type (Fe, Al)Ni nanoprecipitates. *Mater. Today Commun.* **2023**, *36*, 106564. [CrossRef]
14. Liang, H.; He, R.; Liu, L.; Zhang, W.; Fang, L. Investigating the elastic, mechanical, and thermal properties of polycrystalline Mo2C under high pressure and high temperature. *Ceram. Int.* **2023**, *49*, 7341–7349. [CrossRef]
15. Feng, X.; Xue, F.; Zhao, P.; Lu, Y. The electronic structure, elastic properties, dynamical stability and thermoelectric properties of rock-salt and orthorhombic phases of CdS: First-principles calculations. *Solid State Commun.* **2022**, *353*, 114878. [CrossRef]
16. Zhang, F.; Luan, B.; Chu, L.; Wen, S.; Zhang, S.; Wang, Y.; Wu, L.; Murty, K.L. Effects of composition on phase stabilities and elastic properties in TiZrAlV alloys: Experiments and first-principles calculations. *J. Alloys Compd.* **2021**, *863*, 158054. [CrossRef]
17. Mizushima, A.; Isikawa, Y.; Maeda, A.; Oyabe, K.; Mori, K.; Sato, K.; Kamigaki, K. A new dense-kondo compound $CeNiAl_4$. *J. Phys. Soc. Jpn.* **1991**, *60*, 753–756. [CrossRef]
18. Raghavan, V. Al-Ce-Ni (Aluminum-Cerium-Nickel). *J. Phase Equilb. Diff.* **2009**, *30*, 265–267. [CrossRef]
19. Clark, S.J.; Segall, M.D.; Pickard, C.J.; Hasnip, P.J.; Probert, M.J.; Refson, K.; Payne, M.C. First principles methods using CASTEP. *Z. Kristallogr.* **2005**, *220*, 567–570. [CrossRef]
20. Oliver, G.L.; Perdew, J.P. Spin-density gradient expansion for the kinetic energy. *Phys. Rev. A* **1979**, *20*, 397–403. [CrossRef]
21. Kohn, W.; Sham, L.J. Self-consistent equations including exchange and correlation effects. *Phys. Rev.* **1965**, *140*, 1133–1137. [CrossRef]
22. Cava, R.J.; Ramirez, A.P.; Takagi, H.; Krajewski, J.J.; Peck, W.F. Physical properties of some ternary ce intermetallics with the transition metals Ni and Pd. *J. Magn. Magn. Mater.* **1993**, *128*, 124–128. [CrossRef]
23. Isikawa, Y.; Mizushima, T.; Sakurai, J.; Mori, K.; Munoz, A.; Givord, F.; Boucherle, J.; Voiron, J.; Oliveira, I.S.; Flouquet, J. Magnetic properties and neutron diffraction measurements of dense-kondo compound $CeNi_2Al_5$. *J. Phys. Soc. Jpn.* **1994**, *63*, 2349–2358. [CrossRef]
24. Oesterreicher, H. Structural and magnetic studies on rare-earth compounds RNiAl and RCuAl. *J. Less-Common Met.* **1973**, *30*, 225–236. [CrossRef]
25. Gout, D.; Benbow, E.; Gourdon, O.; Miller, G.J. Crystallographic, electronic and magnetic studies of $Ce_4Ni_6Al_{23}$: A new intermetallic compound in the cerium-nickel-aluminum phase diagram. *J. Solid State Chem.* **2003**, *174*, 471–481. [CrossRef]
26. Fang, C.M.; Huis, M.A.; Zandbergen, H.W. Stability and structures of the CFCC-TmC phases: A first-principles study. *Comput. Mater. Sci.* **2012**, *51*, 146–150. [CrossRef]
27. Rougab, M.; Gueddouh, A. First-principles insights into structural stability, elastic anisotropies, mechanical and thermodynamic properties of the Hf2GeX (X = C, N, and B) 211 MAX phases. *J. Phys. Chem. Solids* **2023**, *176*, 111251. [CrossRef]
28. Tang, C.; Du, Y.; Zhou, H. The phase equilibria of the Al–Ce–Ni system at 500 °C. *J. Alloys Compd.* **2009**, *470*, 222–227. [CrossRef]
29. Yang, K.; Wan, R.D.; Zhang, Z.F.; Lei, Y.; Tian, G.C. First-principles investigation on the thermoelectric and electronic properties of HfCoX (X = As, Sb, Bi) half-Heusler compounds. *J. Solid State Chem.* **2022**, *314*, 123386. [CrossRef]
30. Beckstein, O.; Klepeis, J.E.; Hart, G.L.; Pankratov, O. First-principles elastic constants and electronic structure of $\alpha - Pt_2Si$ and PtSi. *Phys. Rev. B* **2001**, *63*, 134112. [CrossRef]
31. Watt, J.P.; Peselnick, L. Elastic properties of polycrystalline minerals: Comparison of theory and experiment. *J. Appl. Phys.* **1980**, *51*, 1525. [CrossRef]
32. Wu, Z.J.; Zhao, E.J.; Xiang, H.P.; Hao, X.F.; Liu, X.J.; Meng, J. Crystal structures and elastic properties of superhard IrN2 and IrN3 from first principles. *Phys. Rev. B* **2007**, *76*, 054115. [CrossRef]
33. Ling, Y.; Liu, W.; Zou, X.; Yan, H. Phase stability and elastic properties of Al–Pr intermetallic compounds from first principles calculations. *Physica B* **2023**, *663*, 415001. [CrossRef]
34. Li, C.; Zhang, X.; Wang, F. First-principles study on the lattice vibration, anisotropy, tensile strength and electronic properties of CuxHfySiz intermetallics. *Chem. Phys. Lett.* **2023**, *830*, 140811. [CrossRef]
35. Pugh, S.F. XCII. Relations between the elastic moduli and the plastic properties of polycrystalline pure metals. *Philos. Mag. Ser.* **1954**, *45*, 823–843. [CrossRef]
36. Li, K.; Wang, X.; Zhang, F.; Xue, D. Electronegativity Identification of Novel Superhard Materials. *Phys. Rev. Lett.* **2008**, *100*, 235504. [CrossRef] [PubMed]
37. KÖSTER, W.; Franz, H. Poisson's ratio for metals and alloys. *Int. Mater. Rev.* **1961**, *6*, 1–56. [CrossRef]
38. Sun, F.; Zhang, G.; Ren, X.; Wang, M.; Xu, H.; Fu, Y.; Tang, Y.; Li, D. First-principles studies on phase stability, anisotropic elastic and electronic properties of Al-La binary system intermetallic compounds. *Mater. Today Commun.* **2020**, *24*, 101101. [CrossRef]
39. Chen, H.; Yang, L.; Long, J. First-principles investigation of the elastic, Vickers hardness and thermodynamic properties of Al–Cu intermetallic compounds. *Superlattices Microstruct.* **2015**, *79*, 156–165. [CrossRef]
40. Wang, H.; Zhou, Y.; Dong, Q.; Chen, X.; Tan, J. First-principles study on the thermodynamic, electronic and mechanical properties of Mg-Al-Si ternary compounds. *J. Mater. Res. Technol.* **2022**, *19*, 2848–2862. [CrossRef]
41. Liao, M.; Liu, Y.; Cui, P. Modeling of alloying effect on elastic properties in BCC Nb-Ti-V-Zr solid solution: From unary to quaternary. *Comput. Mater. Sci.* **2020**, *172*, 109289. [CrossRef]
42. Özer, T. Investigation of pressure dependence of anisotropy and elastic modulus of SbSI compound in ferroelectric phase by Ab initio method. *Mater. Sci. Eng. B* **2023**, *297*, 116787. [CrossRef]

43. Gaillac, R.; Pullumbi, P.; Coudert, F.X. ELATE: An open-source online application for analysis and visualization of elastic tensors. *J. Phys. Condens. Matter.* **2016**, *28*, 275201. [CrossRef] [PubMed]
44. Nong, Z.S.; Zhu, J.C.; Yang, X.W.; Cao, Y.; Lai, Z.H.; Liu, Y. First-principles investigation of the elastic and electronic properties of the binary intermetallics in the Al–La alloy system. *Physica B* **2012**, *407*, 4706–4711. [CrossRef]